Journal of Materials Processing Technology 222 (2015) 206–218

Contents lists available at ScienceDirect

Journal of Materials Processing Technology

journal homepage: www.elsevier.com/locate/jmatprotec

Laser microsculpting for the generation of robust diffractive security markings on the surface of metals

Krystian L. Wlodarczyk[a,*], Marcus Ardron[a,b], Andrew J. Waddie[a], Andrew Dunn[a], Matthew D. Kidd[b], Nicholas J. Weston[b], Duncan P. Hand[a]

[a] Institute of Photonics and Quantum Sciences, School of Engineering and Physical Sciences, Heriot-Watt University, Edinburgh EH14 4AS, United Kingdom
[b] Renishaw plc, Research Park North, Riccarton, Edinburgh EH14 4AP, United Kingdom

ARTICLE INFO

Article history:
Received 7 September 2014
Received in revised form 22 January 2015
Accepted 3 March 2015
Available online 10 March 2015

Keywords:
Laser materials processing
Surface modification
Microstructure fabrication
Diffractive optics
Laser marking
Metals

ABSTRACT

We report the development of a laser-based process for the direct writing (‘*microsculpting*’) of unique security markings (reflective phase holograms) on the surface of metals. In contrast to the common approaches used for unique marking of the metal products and components, e.g., polymer holographic stickers which are attached to metals as an adhesive tape, our process enables the generation of the security markings directly onto the metal surface and thus overcomes the problems with tampering and biocompatibility which are typical drawbacks of holographic stickers. The process uses 35 ns laser pulses of wavelength 355 nm to generate optically-smooth deformations on the metal surface using a localised laser melting process. Security markings (holographic structures) on 304-grade stainless steel surface are fabricated, and their resulted optical performance is tested using a He–Ne laser beam of 632.8 nm wavelength.

1. Introduction

Laser-based melting processes are increasingly used in a variety of industrial (Wissenbach et al., 2011), medical (Temmler et al., 2010) and optical (e.g. Nowak et al., 2006) applications for surface smoothing and polishing. In these processes, the laser beam is used to generate a melt pool on the material surface, enabling the molten layer to flow under surface tension forces, thereby causing surface relaxation and consequently roughness reduction (Wlodarczyk et al., 2010). Typically, however, new surface deformations such as bumps, dimples, corrugations and ripples are also generated during the re-melting and re-solidification process. The appearance of such surface deformations depends on the absorbed laser intensity, temperature gradients generated on the surface and the chemical composition of the material, as explained by Wissenbach et al. (2011). Chen et al. (2000), for instance, observed that deformations in the form of bumps generated on a Ni-P hard disc substrate result from both a change in the surfactant concentration and the thermocapillary (Marangoni) forces which are induced by the temperature gradients occurring across the molten area.

Fibre and solid-state lasers are commonly used for re-melting, polishing and texturing the surface of metals, such as steel (Temmler et al., 2011), titanium (Nusser et al., 2013), GGG70L cast iron (Ukar et al., 2013) and nickel-based Inconel®718 alloy (Kumstel and Kirsch, 2013). Khoong et al. (2010) demonstrated that a 355 nm solid-state YAG laser can also be used for so called “soft marking” of silicon wafers. In the case of transparent materials, such as glass and glass-ceramics, surface polishing and texturing processes are carried out by using a CO_2 laser beam at 10.6 μm because at this wavelength these materials have a high absorption coefficient, enabling the laser light to be coupled more efficiently. For example, it has been demonstrated that a CO_2 laser beam can be successfully used for polishing the surface of conventional refractive optics (Laguarta et al., 1994 and Heidrich et al., 2011) and for smoothing sharp etched-edges of diffractive optical elements (Wlodarczyk et al., 2010). The CO_2 laser irradiation can also be used for the fabrication of micro-optical components, e.g., micro-stripe cylindrical and toroidal mirrors (Wlodarczyk et al., 2012) and phase corrective plates for high power laser diodes, as reported by Nowak et al. (2006), Monjardin et al. (2006) and Trela et al. (2009). A CO_2 laser beam can also be used for texturing the surface of optical glasses, as demonstrated by Shiu et al. (1999) and Bennett et al. (1999), or even for repairing of damage in fused silica components by re-melting, as reported by Mendez et al. (2006) and Cormont et al. (2013). Moreover, Brusasco et al. (2001) and recently

* Corresponding author at: Room EM G24, Heriot-Watt University, Riccarton, Edinburgh EH14 4AS, UK. Tel.: +44 (0) 131 451 3105; fax: +44 (0) 131 451 4155.
E-mail address: K.L.Wlodarczyk@hw.ac.uk (K.L. Wlodarczyk).

http://dx.doi.org/10.1016/j.jmatprotec.2015.03.001
0924-0136/

Dai et al. (2011) demonstrated that CO_2 laser polishing can also enhance surface damage resistance of optical components.

Currently common techniques for marking metals include mechanical processes (e.g. indentation), ink-marking, laser ablation (marking and engraving), electro-marking and etching, which are typically used for the generation of company logos, trademarks, alphanumeric characters (e.g. serial numbers), bar codes, QR codes and data matrices (Dahotre and Harimkar, 2008). All these 'standard' markings, however, can be easily replicated and thus expensive products (e.g. engine components) can be counterfeited. More sophisticated markings like polymer holographic stickers, which are more robust to local damage and counterfeiting, are produced by a mechanical embossing process. Such holograms, however, are not embedded into the metal surface, but rather attached as an adhesive tape, and thus are vulnerable to tampering. Moreover, they reveal biocompatibility problems and thus they cannot be used for marking medical instruments and implants.

The work described in this paper is focused on the development of a process for the generation of small-scale surface features (with a diameter of up to 10 μm and a peak-to-valley value of up to 500 nm) on metals using a localised laser melting process. By creating the deformations in appropriate locations on the metal surface, we generate optically-smooth holographic structures which are directly embedded into the metal. Since such structures can produce a diffraction pattern containing text and images, they simply can be used as security markings for identification and traceability of high value metal components. In this paper, we investigate the generation of laser-induced surface deformations (LISDs) in metals which are commonly used as substrates for manufacturing medical instruments, implants and components in aircraft engines, nuclear reactors and pumps. The LISDs are generated by a pulsed, frequency-tripled solid-state laser which provides 35 ns pulses at a 10 kHz pulse repetition frequency in UV ($\lambda = 355$ nm). Based on our previous work, which was reported by Weston et al. (2012), this laser is capable of producing optically-smooth deformations with the peak-to-valley value of 200 ± 20 nm on the surface of different metals, such as a 316-grade stainless steel and martensitic chromium steel Sandvik Chromflex®. In this paper, we analyse the evolution of the LISDs in terms of the applied laser pulse energy (average power) and the number of laser pulses and identify the laser processing parameters which can be used to generate optically-smooth surface features with a good control over their depth or height.

2. Interaction of UV nanosecond laser pulses with metals

Four different metals, austenitic 304-grade stainless steel, 99% pure nickel and two nickel-chromium alloys (Inconel®625 and Inconel®718 alloy) were investigated. The stainless steel samples were 0.35 mm thick, whereas the thickness of the other samples was 2 mm. The metal surfaces were mechanically polished before the laser treatment. The metal samples after polishing were measured to have an average surface roughness Ra < 6 nm and RMS (Rq) < 10 nm in a 0.34 mm by 0.26 mm measured window.

A detailed analysis of the laser-induced surface deformations (LISDs) generated by the nanosecond pulses in UV was performed using a white-light source interferometer (Zygo) and an atomic force microscope (Digital Instruments Veeco). These instruments measured the LISDs with a lateral (spatial) resolution of <0.2 μm and a vertical resolution of ≤1 nm. Based on the surface profiles, the diameter, peak-to-valley value and level (depth/height) of the central area of the LISDs were determined for different values of the pulse energy (average laser power) and number of laser pulses.

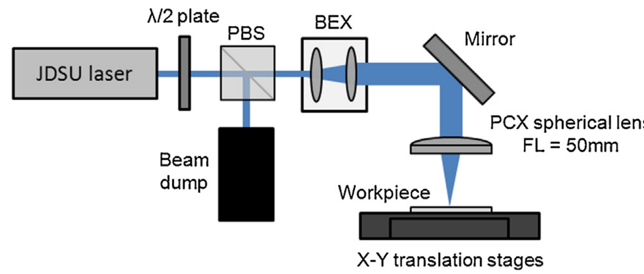

Fig. 1. Schematic of the experimental setup.

2.1. Experimental setup

The optical setup used in the experiments described below is shown in Fig. 1. The laser source is a 10 W Q-switched diode-pumped UV laser (JDSU Q-series) which provides 35 ns pulses (FWHM) with a 10 kHz pulse repetition frequency. A 1.6 mm diameter laser beam (measured at $1/e^2$ of its maximum intensity) with $M^2 < 1.2$ is delivered to the workpiece via a half-wave ($\lambda/2$) plate, polarising beam splitter (PBS) cube, a ×3 beam expander (BEX) and a conventional plano-convex (PCX) spherical lens of 50 mm focal length. The focused laser beam diameter on the workpiece ($2\omega_o$) was calculated to be 8 ± 1 μm (at $1/e^2$ of its maximum intensity) using the following equation:

$$\omega_o = \frac{M^2 \cdot FL \cdot \lambda}{\pi \cdot \omega_I} \quad (1)$$

where FL is the focal length of the PCX spherical lens (50 mm), λ is the laser wavelength (355 nm), and ω_I is the radius of the expanded laser beam which was measured to be 2.6 mm (at $1/e^2$ of its maximum intensity). The M^2 value of the laser beam after BEX was measured to be approximately 1.8. The calculated focused laser beam diameter is similar to the diameter of LISDs observed in the studied metals (see Sections 2.2–2.5). It was not possible to directly measure the focused laser beam using a beam-profiling camera (e.g. Spiricon) because the laser spot size is similar to the camera resolution.

Laser processing is carried out by moving the workpiece using two motorised linear stages. When the workpiece is settled in a desired position, the laser delivers a pre-defined number of laser pulses at fixed energy to the target. The stages ensure the workpiece movement with a 0.5 μm resolution. The maximum average laser power (pulse energy) delivered to the workpiece was manually controlled by rotating the $\lambda/2$ plate, whereas very accurate adjustment (with a 1% resolution of the maximum average power) was carried out using the laser software.

2.2. 304-grade stainless steel

Austenitic 304-grade stainless steel is the most versatile and widely used stainless steel. This metal contains at least 66% Fe, 17.5–19.5% Cr, 8–10.5% Ni, up to 2% Mn, up to 1% Si and some traces of C, P and S.

In general, it was found that the UV ns laser pulses generate repeatable and useful structures on the 304-grade stainless steel. This was not the case for the longer wavelengths (1030 nm and 515 nm) where the degree of depth control is much reduced and the generated surface is significantly rougher. In the range of laser pulse energies (E_p) between 1.5 and 4.5 μJ, the LISDs were observed in the form of smooth '*Gaussian-like*' craters with an elevated rim. Fig. 2 shows examples of such deformations. Craters with a depth of >0.7 μm were produced when E_p > 4.5 μJ. Such deep craters are not discussed further because they are beyond the scope of our interest.